



OPEN ACCESS

## ORIGINAL RESEARCH

# Homozygous mutations in *DZIP1* can induce asthenoteratospermia with severe MMAF

Mingrong Lv,<sup>1,2,3</sup> Wangjie Liu,<sup>4,5,6</sup> Wangfei Chi,<sup>7</sup> Xiaoqing Ni,<sup>1,2,3</sup> Jiajia Wang,<sup>1,2,3</sup> Huiru Cheng,<sup>1,8,9</sup> Wei-Yu Li,<sup>4,5,6</sup> Shenmin Yang,<sup>10</sup> Huan Wu,<sup>1,8,9</sup> Junqiang Zhang,<sup>1,8,9</sup> Yang Gao,<sup>1,2,3</sup> Chunyu Liu,<sup>4,5,6</sup> Caihua Li,<sup>11</sup> Chenyu Yang,<sup>12</sup> Qing Tan,<sup>1,8,9</sup> Dongdong Tang,<sup>1,8,9</sup> Jingjing Zhang,<sup>1,8,9</sup> Bing Song ,<sup>1,8,9</sup> Yu-Jie Chen,<sup>1,8,9</sup> Qiang Li,<sup>1,8,9</sup> Yading Zhong,<sup>13</sup> Zhihua Zhang,<sup>14</sup> Hexige Saiyin,<sup>4</sup> Li Jin,<sup>4</sup> Yuping Xu,<sup>1,8,9</sup> Ping Zhou,<sup>1,8,9</sup> Zhaolian Wei,<sup>1,8,9</sup> Chuanmao Zhang,<sup>7</sup> Xiaojin He ,<sup>1,2,3</sup> Feng Zhang ,<sup>4,5,6</sup> Yunxia Cao<sup>1,2,3</sup>

► Additional material is published online only. To view please visit the journal online (<http://dx.doi.org/10.1136/jmedgenet-2019-106479>).

For numbered affiliations see end of article.

## Correspondence to

Associate Professor Xiaojin He; [hxj0117@126.com](mailto:hxj0117@126.com)  
Professor Feng Zhang; [zhangfeng@fudan.edu.cn](mailto:zhangfeng@fudan.edu.cn)  
Professor Yunxia Cao; [caoyunxia6@126.com](mailto:caoyunxia6@126.com)

ML, Wal, WC and NX contributed equally.

Received 2 August 2019  
Revised 2 December 2019  
Accepted 21 December 2019



© Author(s) (or their employer(s)) 2020. Re-use permitted under CC BY-NC. No commercial re-use. See rights and permissions. Published by BMJ.

**To cite:** Lv M, Liu W, Chi W, et al. *J Med Genet* Epub ahead of print: [please include Day Month Year]. doi:10.1136/jmedgenet-2019-106479

## ABSTRACT

**Background** Asthenoteratospermia, one of the most common causes for male infertility, often presents with defective sperm heads and/or flagella. Multiple morphological abnormalities of the sperm flagella (MMAF) is one of the common clinical manifestations of asthenoteratospermia. Variants in several genes including *DNAH1*, *CEP135*, *CATSPER2* and *SUN5* are involved in the genetic pathogenesis of asthenoteratospermia. However, more than half of the asthenoteratospermia cases cannot be explained by the known pathogenic genes.

**Methods and results** Two asthenoteratospermia-affected men with severe MMAF (absent flagella in >90% spermatozoa) from consanguineous families were subjected to whole-exome sequencing. The first proband had a homozygous missense mutation c.188G>A (p.Arg63Gln) of *DZIP1* and the second proband had a homozygous stop-gain mutation c.690T>G (p.Tyr230\*). Both of the mutations were neither detected in the human population genome data (1000 Genomes Project, Exome Aggregation Consortium) nor in our own data of a cohort of 875 Han Chinese control populations. *DZIP1* encodes a DAZ (a protein deleted in azoospermia) interacting protein, which was associated with centrosomes in mammalian cells. Immunofluorescence staining of the centriolar protein Centrin1 indicated that the spermatozoa of the proband presented with abnormal centrosomes, including no concentrated centriolar dot or more than two centriolar dots. HEK293T cells transfected with two *DZIP1*-mutated constructs showed reduced DZIP1 level or truncated DZIP1. The *Dzip1*-knockout mice, generated by the CRISPR-Cas9, revealed consistent phenotypes of severe MMAF.

**Conclusion** Our study strongly suggests that homozygous *DZIP1* mutations can induce asthenoteratospermia with severe MMAF. The deficiency of DZIP1 induces sperm centrioles dysfunction and causes the absence of flagella.

## INTRODUCTION

Infertility prevents millions of couples from natural conception, thus becoming a major healthy concern.<sup>1</sup> Asthenoteratospermia is characterised

by decreased sperm motility and obvious morphological abnormalities in sperm head, neck or flagella, causing male infertility.<sup>2–3</sup> As early as 2003, homozygous partial deletion in *CATSPER2* (MIM: 607249) was first described to be associated with infertility phenotype with abnormal sperm motility and morphology in humans.<sup>4</sup> Till now, several genes responsible for different types of asthenoteratospermia have been identified. For example, biallelic *SUN5* (MIM: 613942) mutations cause severe acephalic spermatozoa.<sup>5</sup> *DNAH1* (MIM: 603332), *CFAP* family members and some other genes have been reported to induce human multiple morphological abnormalities of the flagella (MMAF).<sup>2–21</sup> Mutations in *AURKC* and *DYP19L2* account for most cases of macrozoospermia and globozoospermia, respectively.<sup>22–26</sup> These findings demonstrated that asthenoteratospermia has strong genetic heterogeneity and diverse phenotypes.

The centrosome consists of two centrioles, pericentriolar material and centriolar satellites, and is involved in numerous functions such as organisation of the mitotic and meiotic spindle.<sup>27–31</sup> During flagellum biogenesis, the flagellar axoneme originates from the sperm centrioles located at the basal bodies.<sup>32</sup> Moreover, during human fertilisation, the sperm centrosome organises the sperm aster, which is essential to unite the sperm and oocyte pronuclei, and controls the first mitotic divisions after fertilization.<sup>33–34</sup> Therefore, it could be speculated that defects in the proteins shared between sperm centrosome and flagella may disturb the flagellar formation, meiosis and first mitotic divisions after fertilisation.

In this study, by using whole-exome sequencing (WES), homozygous mutations of *DZIP1* (DAZ interacting zinc finger protein 1, MIM: 608671) were identified in two unrelated Han Chinese men affected with asthenoteratospermia, who did not carry bi-allelic pathogenic mutations in any of those known genes. The mammalian *DZIP1* gene encodes a zinc finger and coiled-coil containing protein, which interacts with the DAZ (deleted in azoospermia) protein,<sup>35</sup> and is predominantly expressed in testis. Mouse DZIP1 and its zebrafish homologue protein (Iguana) have previously been

reported to be associated with centrosomes and ciliogenesis in cells.<sup>36–38</sup> Notably, the two *DZIP1*-mutated probands consistently presented severe MMAF with predominantly high malformation rates of absent flagella (>90%). The absence of *DZIP1* and abnormal signals of centrioles were observed in the spermatozoa from both probands. In parallel, we characterised a *Dzip1*-knockout mouse model, which resembled the severe MMAF phenotypes. Overall, our study strongly suggests that *DZIP1* is required for the formation of both sperm flagella and sperm centrioles, and that homozygous *DZIP1* mutation can induce asthenoteratospermia with severe MMAF.

## MATERIALS AND METHODS

### Subjects and clinical investigation

A cohort of 65 unrelated Han Chinese man preliminarily diagnosed with MMAF were recruited from the First Affiliated Hospital of Anhui Medical University and the Affiliated Suzhou Hospital of Nanjing Medical University in China. Some patients in this cohort were previously described.<sup>10 16 17 19 39 40</sup> All 65 men suffered from primary infertility for more than 1 year. Two probands in this study were from consanguineous families. Their ages were 27 (A029 IV-1) and 28 (A0033 IV-1), respectively. No obvious symptoms of other ciliopathies (such as primary cilia dyskinesia, polycystic kidney disease or Bardet–Biedl syndrome) were observed in the two probands by careful clinical examinations (online supplementary figure S1). The two probands will be followed up constantly. The karyotype analysis performed in two cases showed normal somatic karyotypes (46; XY) and no large-scale deletions in the human Y chromosome. Informed consents were obtained from each subject.

Semen analyses were carried out during routine examination of the individuals according to the WHO guideline (the fifth Edition). Sperm morphology was assessed by modified Papanicolaou staining. At least 200 spermatozoa were examined. The percentages of morphologically abnormal spermatozoa were evaluated according to the WHO guidelines.

### WES, bioinformatic analysis and Sanger sequencing

WES and bioinformatic analysis were performed according to our previously described protocols.<sup>8</sup> *DZIP1* mutations identified by WES were validated by Sanger sequencing. PCR primers and protocols used for each individual are listed in online supplementary table S1.

### Expression vector construction, cell culture and transfection

To construct the wild-type (WT) and two *DZIP1*-mutated (p.Arg63Gln and p.Tyr23\*) expression plasmids, total RNA was extracted from testicular tissues of the control subject with obstructive azoospermia, and was reverse-transcribed to cDNA. The full-length cDNA was amplified, respectively, by full-length PCR and segmental PCR that induced mutations (primer sequences were provided in online supplementary table S2). Then the amplification was inserted into the pEGFP-C1 vector between the restriction sites of *Bgl*II and *Bam*HI. HEK293T cells were cultured in DMEM medium supplemented with 10% Fetal bovine serum (Invitrogen) and 1% antibiotics (100 units/mL penicillin and 100 µg/mL streptomycin, Invitrogen) at 37°C and 5% CO<sub>2</sub>. The empty and recombinant plasmids were transfected into HEK293T cells using Lipofectamine 3000 (Invitrogen) according to the manufacturer's recommendations.

### Western blotting

Transfected cells and half of a mouse testis were homogenised in 200 µL RIPA (Beyotime) using a pellet pestle motor homogeniser and then heated at 100°C for 15 min. Lysates were fractionated by SDS-PAGE on 10% polyacrylamide gels, transferred to polyvinylidene fluoride membranes, and the membranes were blocked in TBST (3% Bovine serum albumin in tris-buffered saline with Tween-20) for 1 hour at room temperature (RT). Anti-*DZIP1* antibody (mouse monoclonal, Santa Cruz) was diluted 1:1000 in TBST and incubated with the membranes overnight at 4°C. ECL (Kodak) was used for visualisation. Protein levels were normalised using the reference protein GAPDH.

### Transmission electron microscopy

Sample preparation of the human sperm for routine transmission electron microscopy (TEM) has been previously described.<sup>17</sup> In this study, more than 1000 sections were observed to investigate the longitudinal sections of sperm and confirm the phenotype of absent axoneme.

### Generation of *Dzip1*-knockout mouse model

*Dzip1*-knockout mice were generated by Nanjing Biomedical Research Institute of Nanjing University according to our previously published protocol.<sup>10</sup> The single-guide RNA (sgRNA) was designed against *Dzip1* exon 2. The frameshift mutation in *Dzip1* was identified in founder mice and their offspring by Sanger sequencing (the primer information was provided in online supplementary table S3). All experiments involving mice were performed according to the methods approved by the Animal Ethics Committees of each corresponding institution.

### Mouse histology

Fresh mouse testis and epididymis were fixed in modified Davidson's fluid (50% diluted water, 30% formaldehyde, 15% ethanol and 5% glacial acetic acid), respectively, for over 48 hours. After fixed, the tissues were dehydrated in the gradient alcohol (70% ethanol for 24 hours, 80% ethanol for 2 hours, 90% ethanol for 2 hours and 100% ethanol for 1 hour). Then, the tissues were placed in xylene for 1 hour, and finally embedded in paraffin wax and sectioned to ~4 µm.

For haematoxylin and eosin staining, sections deparaffinised in xylene at 65°C overnight. After deparaffinisation, slides were stained with hematoxylin and eosin, dehydrated and mounted.

### Immunofluorescence staining

Immunofluorescence experiments were performed using human spermatozoa and mice testes as previously described.<sup>10</sup> Briefly, human spermatozoa were coated on the slides and fixed in cold methanol for 5–10 min. The slides were soaked (3% Bovine serum albumin and 0.1% Triton X-100 in 1× phosphate-buffered saline (PBS)) at RT for 1 hour and then incubated overnight at 4°C with the following primary antibodies: rabbit polyclonal anti-*DZIP1* (Abgent, targeting 568–596 amino acids of human *DZIP1* protein), rabbit polyclonal anti-IFT88 (Proteintech), rabbit polyclonal anti-IFT140 (Proteintech) and rabbit polyclonal anti-Centrin1 (Proteintech). After that, slides were washed by 1×PBS three times for ten minutes at a time, followed by 1-hour incubation at RT with secondary antibodies (AlexaFluor 647 anti-Rabbit, Yeasen; AlexaFluor 488 anti-Mouse, Invitrogen) and 0.5% 4',6-diamidino-2-phenylindoles (DAPI).

For immunofluorescence staining of mouse testis, after being carefully deparaffinised and rehydrated, the tissue sections were put into boiled 10 mM citrate buffer (pH 6.0) for 10 min and

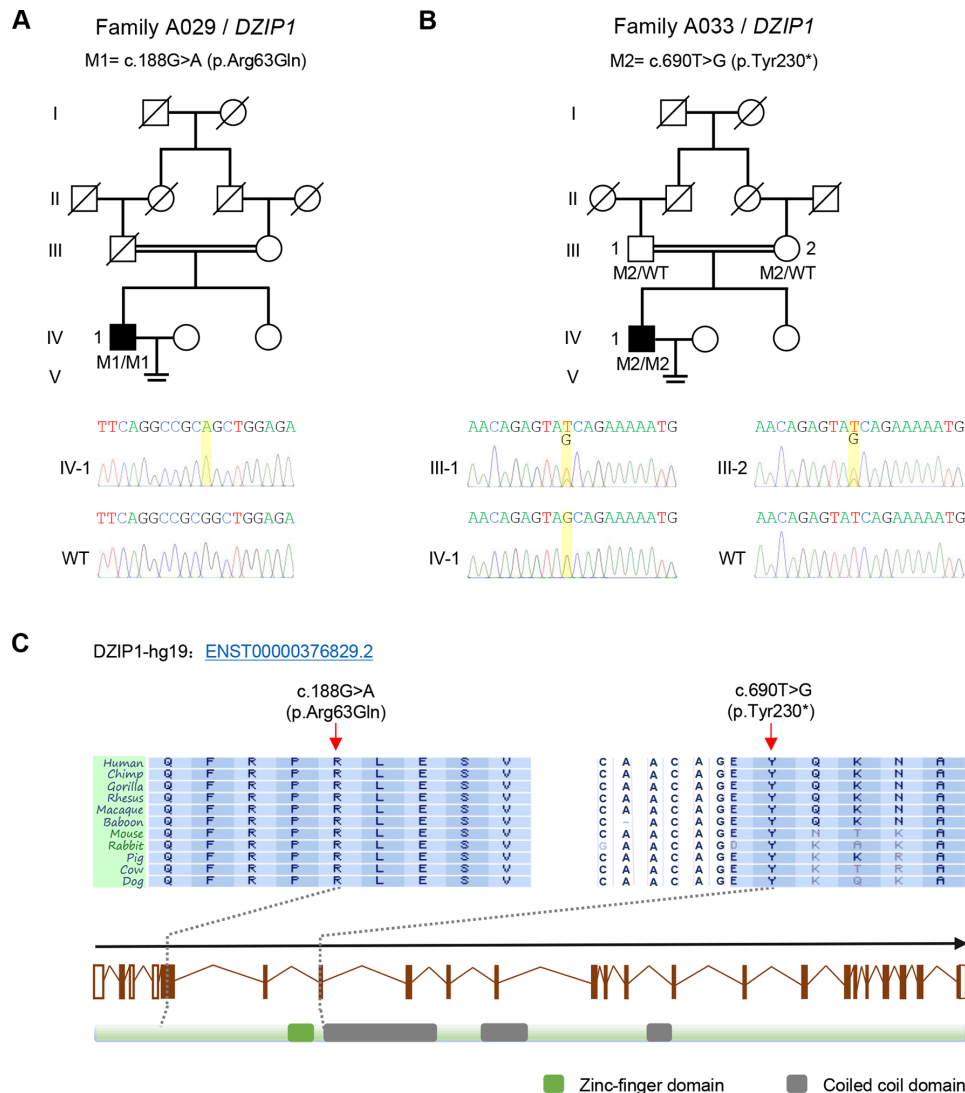


**Figure 1** Homozygous *DZIP1* mutations identified in men with asthenoteratospermia. (A) A missense mutation c.188G>A (p.Arg63Gln) of *DZIP1* was identified in the consanguineous family A029. The proband (IV-1) was homozygous for this mutation (M1). (B) A stop-gain mutation c.690T>G (p.Tyr230\*) of *DZIP1* was identified in the consanguineous family A033. This mutation (M2) was homozygous in the proband (IV-1), and was confirmed to be inherited from his parental heterozygous carriers. (C) These two *DZIP1* mutations (M1 and M2) are located at the conserved sites close to the N-terminal. Green and grey squares, respectively, stand for zinc-finger domain and coiled-coil domains as described by the UniProt server. Both mutations were verified by Sanger sequencing. The mutation positions are indicated by yellow boxes. Mutations are annotated in accordance to the Human Genome Variation Society's recommendations. WT, wild type.

were then treated with 0.1% Triton X-100 in PBS for 30 min. After blocking non-specific binding sites with 10% normal donkey serum (Jackson ImmunoResearch Labs), the slides were incubated with mouse monoclonal anti-*DZIP1* (Santa Cruz) at 4°C overnight, and with AlexaFluor 647 anti-Rabbit and 0.5% DAPI for two additional hours at RT. Slides of both sperm and testicular tissues were observed with an LSM800 confocal microscope (Carl Zeiss AG).

### Mating test

Fertility was investigated in the male mice (8–12 weeks, n=6) of WT, heterozygous and homozygous *Dzip1* mutations. Each male mouse was caged with two WT C57BL/6J females (8–12 weeks), and vaginal plugs were checked every morning. Once a vaginal plug was identified, the male mouse was allowed to rest for 2 days before another female mouse was placed in the cage. The mated female mouse was separated and single caged, and the pregnancy results were recorded. The fertility test lasted for 3 weeks.

## RESULTS

### Identification of homozygous *DZIP1* mutations in men with severe MMAF

After WES, stringent bioinformatic filtering analysis and Sanger sequencing, we identified homozygous mutations of *DZIP1* in two Han Chinese men affected with asthenoteratospermia (figure 1 and online supplementary table S4). The proband IV-1 in the consanguineous family A029 had a homozygous missense mutation c.188G>A (p.Arg63Gln) of *DZIP1* (figure 1A). This missense mutation altered a highly conserved amino acid of *DZIP1* protein (figure 1C), and was predicted to be potentially deleterious by all three functional prediction tools: SIFT, PolyPhen-2 and MutationTaster. In the other consanguineous family A033, a homozygous stop-gain mutation c.690T>G (p.Tyr230\*) of *DZIP1* was identified in proband IV-1 and both parents are heterozygous carriers (figure 1B). This mutation was located at the beginning of the first coiled-coil domain of *DZIP1* protein,



## Genotype-phenotype correlations

**Table 1** Semen characteristics in men with homozygous *DZIP1* mutations

Semen parameters*	Human subject				Normal value of WHO criteria
	A029 iv-1		A033 iv-1		
	Test 1	Test 2	Test 1	Test 2	
Semen volume (mL)	6.5	7.0	1.7	2.0	>1.5
Sperm concentration (10 <sup>6</sup> /mL)	3.2	2.8	5.3	0.7	>15.0
Total sperm number (10 <sup>6</sup> /ejaculate)	20.8	19.6	9.0	1.4	>39.0
Motility (%)	0.0	0.0	2.1	0.0	>32.0
Progressive motility (%)	0.0	0.0	0.0	0.0	>40.0

\*The normal values of semen parameters were according to the WHO (2010) manual criteria. Semen analyses were performed twice for each subject.

leading to absence of three coiled-coil domains, which are potentially important in protein-protein interactions. As shown in online supplementary table S4, the two *DZIP1* mutations were absent from the human population datasets of the 1000 Genomes Project, the Exome Aggregation Consortium and the Genome Aggregation Database. We also investigated a Han Chinese control population consisting of 300 fertile Han Chinese individuals and 668 non-MMAF-affected cases. Notably, both *DZIP1* mutations were also absent from the ethnically matched control population (online supplementary table S4). For both probands, no variants with low frequencies in control populations were identified in other genes reported to be associated with cilia, flagella or male infertility. Therefore, *DZIP1* appeared to be a new gene involved in MMAF.

In vitro effects of these two homozygous *DZIP1* mutations were also investigated in HEK293T cells transfected with WT or *DZIP1*-mutated constructs. As shown in online supplementary figure S2, the expression level of *DZIP1* was obviously reduced for the p.Arg63Gln mutation, and *DZIP1* was truncated for the p.Tyr230\* mutation.

### Asthenoteratospermia with severe MMAF in men with homozygous *DZIP1* mutations

The detailed phenotypes in two probands with homozygous *DZIP1* mutations were analysed. Semen analysis showed that the sperm concentration was decreased compared with the standard value of WHO (table 1). The spermatozoa of both probands consistently presented as immotile (table 1). Moreover, no spermatozoa with normal morphology could be observed in any of the two *DZIP1*-mutated men (table 2) under light microscopy. Compared with the spermatozoa from a control sample, various morphological abnormalities of spermatozoa from *DZIP1*-mutated men were observed, such as short and absent flagella (figure 2). Notably, the major flagellar malformation in *DZIP1*-mutated men was absent flagella, accounting for more than 90% spermatozoa, which was obviously higher than those of

**Table 2** Sperm morphology in *DZIP1*-mutated men

Sperm morphology	<i>DZIP1</i> -mutated men* (n=2)	Control men (n=5)
Normal flagella (%)	0 (0–0)	60.2±6.1
Absent flagella (%)	95.7 (92.4–99.0)	2.0±1.1
Short flagella (%)	4.3 (1.0–7.6)	5.0±1.7
Coiled flagella (%)	0 (0–0)	17.8±3.0
Bent flagella (%)	0 (0–0)	16.2±4.6
Irregular flagella (%)	0 (0–0)	0.8±0.8

\*Values represent the mean (range). Five control men were fertile donors who were enrolled from the Anhui Human Sperm Bank.

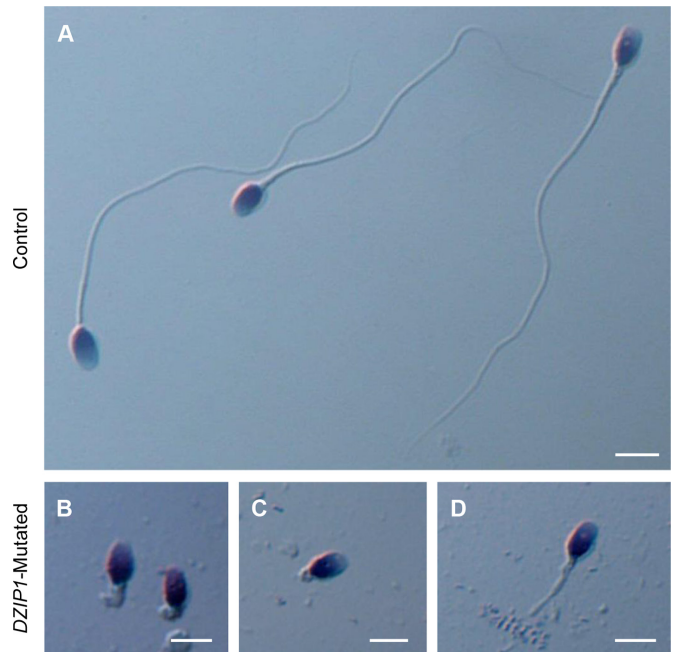


**Figure 2** Sperm morphology in *DZIP1*-mutated men. (A) Normal morphology of a spermatozoon from a healthy control man. (B) to (D) Most spermatozoa of *DZIP1*-mutated men presented multiple morphological abnormalities, such as very short flagella (B), absent flagella (C) and short flagella (D). scale bar: 5  $\mu$ m.

the control fertile men (table 2). In addition, the severe flagellar abnormalities were confirmed by TEM analysis (online supplementary figure S3). Compared with the normal connecting piece and axoneme in the spermatozoon of a control subject, the longitudinal sections of the spermatozoa from the *DZIP1*-mutated men presented with absent or very short axoneme.

### Location of *DZIP1* in sperm head and neck, and *DZIP1* loss in flagellar and centrosomal malformations

To further investigate the pathogenicity of the identified *DZIP1* variants, the localization of *DZIP1* and the intraflagellar transport (IFT) proteins (eg, IFT88 and IFT140) in spermatozoa from control and two *DZIP1*-mutated men were detected by immunofluorescence staining (figure 3). In a spermatozoon from the control individual, the *DZIP1* immunostaining was concentrated in sperm head and neck, and the immunostaining of IFT88 and IFT140 was observed in sperm head and tail. Normal axoneme was presented by the staining of acetylated- $\alpha$ -tubulin. However, the spermatozoon from two probands had no organised axoneme and *DZIP1* immunostaining. The immunostaining of IFT88 and IFT140 was weak or misplaced in sperm head, and absent in sperm tail.

As mentioned above, *DZIP1* has been reported to be associated with centrosomes. To investigate whether *DZIP1* deficiency affects centrosomes, immunofluorescence staining of the centriolar protein Centrin1 was carried out (figure 4). In spermatozoa of a control individual, two angled centriolar dots were observed in sperm neck, and the distal one connected with axoneme. Interestingly, the spermatozoa of proband A033 IV-1 presented the abnormalities including two centriolar dots with abnormal angle, no concentrated dot, or more than two centriolar dots. None of the *DZIP1*-mutated spermatozoa had well-shaped axonemes. Centriolar dots were counted for one hundred spermatozoa in each individual (figure 4B to D). More than half of spermatozoa had abnormal numbers of centrioles in

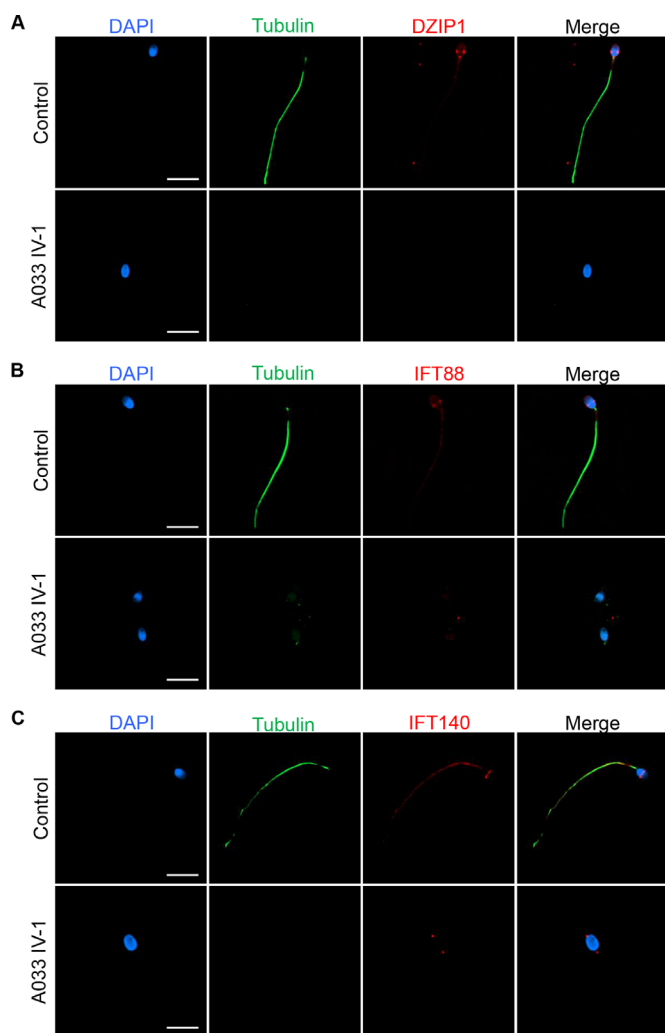


**Figure 3** Immunostaining of DZIP1, IFT88 and IFT140 in human spermatozoa from a healthy control and *DZIP1*-mutated men. (A) In the fertile control, DZIP1 immunostaining (red) was concentrated in sperm head and sperm neck. However, DZIP1 immunostaining was absent in the spermatozoa from *DZIP1*-mutated men. (B) IFT88 immunostaining (red) was observed in sperm head and flagellum in the control subject whereas it was dispersive or absent in the spermatozoa from *DZIP1*-mutated men. (C) IFT140 immunostaining (red) was observed in the middle of sperm head and the flagellum in the control subject, but it was abnormally located in the top of sperm head and sperm neck of the spermatozoa from *DZIP1*-mutated men. Abnormal axonemes (very short or absent flagella) were showed by abnormal acetylated- $\alpha$ -tubulin staining (A to C, green). All these observations of immunostaining were consistent in the spermatozoa of the two *DZIP1*-mutated men. scale bar: 10  $\mu$ m.

subject A033 IV-1 with *DZIP1* deficiency, which was a significant increase when compared with that in the control.

### Consistent asthenoteratospermia phenotypes in *Dzip1*-knockout male mice

To investigate the impact of *DZIP1* deficiency on spermatogenesis, a frameshift mutation (c.102\_132del) was generated in mouse ortholog *Dzip1* using the CRISPR-Cas9 technology (online supplementary figure S4A). This *Dzip1* mutation was predicted to cause premature translational termination (p.Ala-35Serfs\*13) (online supplementary figure S4A), which is closer to *DZIP1* N-terminus. Western blotting and immunofluorescence

using mouse testes confirmed the absence of DZIP1 in *Dzip1*-knockout male mice (*Dzip1*<sup>-/-</sup>) (online supplementary figure S4B, C). The DZIP1 staining was detected in germ cells, especially in elongated spermatids, from the testicular tissue of the WT male mice (online supplementary figure S4C), suggesting that DZIP1 is implicated in spermatogenesis.

Remarkably, all the *Dzip1*<sup>-/-</sup> male mice were infertile (figure 5A). Therefore, the reproductive phenotypes of *Dzip1*-mutated male mice were carefully examined (figure 5). Few spermatozoa from epididymides of the *Dzip1*<sup>-/-</sup> male mice were collected (figure 5B), and no motile spermatozoa was observed (figure 5C). Very few epididymal spermatozoa were observed under light microscope after concentration, presenting severe morphological abnormalities mainly with absent flagella, which were consistent with the phenotypes observed by haematoxylin and eosin staining in testis and epididymis (figure 5D). Moreover, no obvious difference of above reproductive phenotypes was observed between the heterozygous mutated (*Dzip1*<sup>+/-</sup>) male mice and the WT male mice (figure 5).

### DISCUSSION

As mentioned above, we identified homozygous *DZIP1* mutations in 2 (3.1%) out of 65 unrelated Han Chinese men affected with asthenoteratospermia. Notably, there are obvious differences in semen parameters and sperm morphology between *DZIP1*-mutated men and the reported asthenoteratospermia cases in our cohort. The total sperm counts of the two *DZIP1*-mutated patients were obviously decreased (less than 21 million/ejaculate), while those of the patients with other mutations were reduced in only a portion of cases, or even totally normal. Remarkable reductions in sperm motility (less than 22%) and progress motility (less than 10%) were observed among all the *DZIP1*-mutated and reported MMAF patients in our cohort. In addition, the extremely high proportion (90%) of absent flagella, which were confirmed through the absence of Tubulin immunostaining and the sperm TEM analysis of longitudinal sections, were identified in the spermatozoa of both *DZIP1*-mutated men, whereas short flagella were frequently observed in the spermatozoa of *FSIP2*-mutated (82%) and *TTC21A*-mutated patients (more than 63%).<sup>16 17</sup> Besides, the patients with other gene deficiencies (including *CFAP43*-mutated, *CFAP44*-mutated, *CFAP69*-mutated, *CFAP251*-mutated, *DNAH1*-mutated and *SPEF2*-mutated men) presented multiple malformation of flagella (eg, absent, short and/or coiled flagella) without extreme priority in one specific morphology.<sup>10 19 39 40</sup> Furthermore, sperm TEM analyses also revealed the different patterns of ultrastructural abnormalities in sperm among different mutated men. The sperm of *DZIP1*-mutated men mostly presented with absent or very short axoneme, which led to the technical challenge in observing cross-sections of the axoneme. While the majority of the patients with other gene deficiencies in our cohort had observable cross-sections, which presented with relatively minor abnormalities, such as disorganisation or absence of central-pair microtubules, peripheral microtubule doublets and fibrous sheaths.<sup>10 16 17 19 39 40</sup> The characteristic of severe flagellar malformation in *DZIP1*-mutated men, thus, reveals a reasonable speculation that *DZIP1* may have different actions from previously known asthenoteratospermia-associated genes and its deficiency can lead to severe MMAF phenotypes.

Previous studies in zebrafish embryos<sup>41 42</sup> showed that DZIP1 homologue protein (Iguana) localised to the base of primary and motile cilia and was closely associated with the basal bodies. The absence of Iguana completely inhibited the formation of ciliary

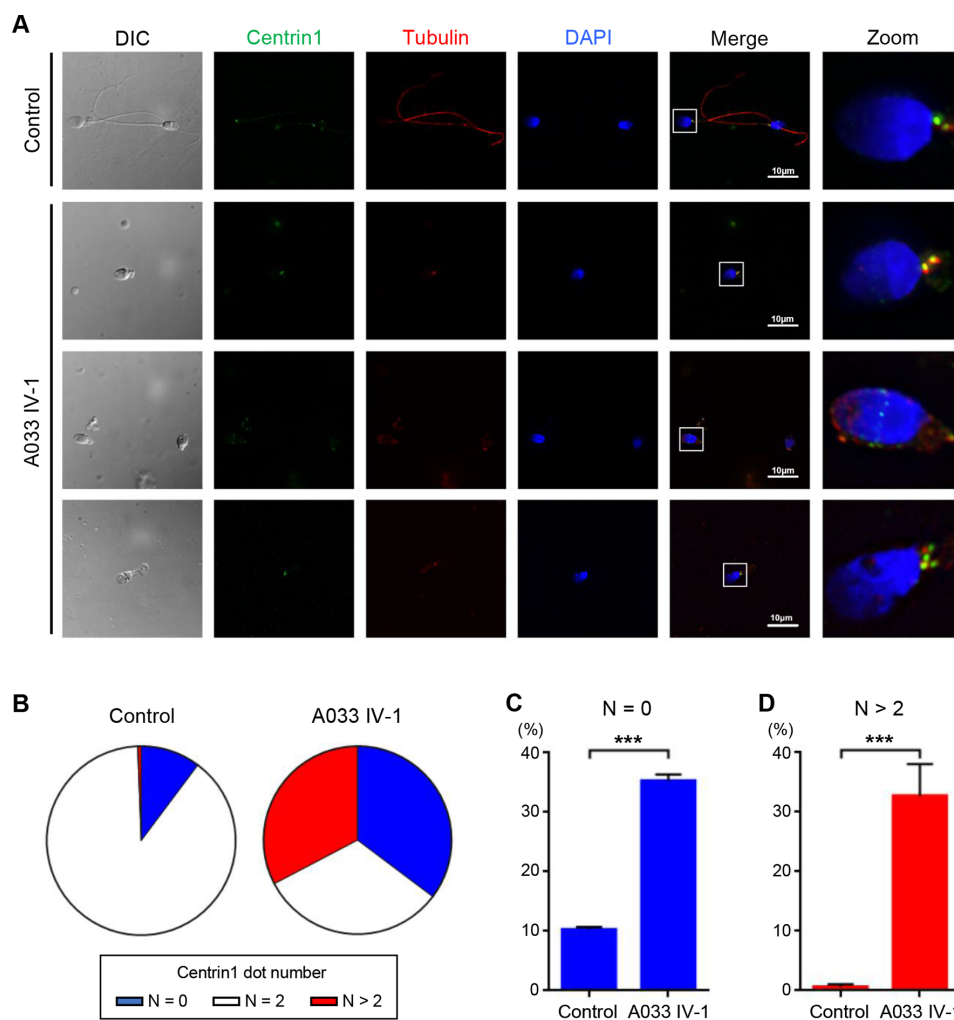


**Figure 4** Immunofluorescence staining of centrioles in spermatozoa from the *DZIP1*-mutated proband A033 IV-1. (A) Spermatozoa from a healthy control man and the proband A033 IV-1 were stained with anti-Centrin1 (green) and anti-acetylated tubulin (red) antibodies. DNA was counterstained with 0.5% DAPI. In the control subject, two angled centriolar dots were observed in sperm neck, and the distal one connected with axoneme. Most spermatozoa of the proband A033 IV-1 presented two centriolar dots with abnormal angle, no concentrated dot, or more than two centriolar dots, and none of them had the well-shaped axoneme. scale bar: 10  $\mu$ m. (B) to (D) More than 100 spermatozoa from each subject were used for counting Centrin1 dots. In the proband A033 IV-1, more than half of spermatozoa had abnormal numbers of centrioles, and the proportion of spermatozoa with abnormal numbers ( $n=0$  and  $n>2$ ) of Centrin1 dots was significantly higher than that in the control subject.

pits and consequently the axonemal outgrowth.<sup>43</sup> As well, in the mouse *Dzip1*-mutated embryonic fibroblasts lacking primary cilia, both Cep164 and Ninein appendage proteins failed to localise to ciliary appendages, and IFT components (eg, Ift88 and Ift140) were not recruited to basal bodies.<sup>36</sup> Furthermore, in our study, few immunofluorescence signals of tubulin were observed in spermatozoa of *DZIP1*-mutated men, and immunofluorescence staining signals of IFT88 and IFT140 were also undetected in sperm tails (figure 3). These studies consistently suggest that *DZIP1* plays a critical role in the early primary ciliogenesis and/or spermiogenesis, and *DZIP1* deficiency can lead to severe arrests of ciliary/flagellar formation. Besides, *DZIP1* is also widely expressed in brain, ovary, kidney and other tissues in addition to testis. Although these two *DZIP1*-mutated men preliminarily presented with primary infertility without obvious phenotypes of other ciliopathies (online supplementary figure S1), the potential and late-onset abnormalities cannot be readily excluded. The follow-up survey and examination should be conducted continuously for long.

In addition, the relationship between *DZIP1* and centrosomes has been hinted before. In mammalian cells, *DZIP1* acting as a centrosome protein, mediates assembly of the BBSome-*DZIP1*-PCM1 complex in the centriolar satellites and regulates the centriolar satellite localisation of the BBSome protein during the cell cycle.<sup>37</sup> Centriolar satellites are small, microscopically visible granules that cluster around centrosomes as several vehicles for protein trafficking.<sup>44</sup> These granules contain numerous proteins, including above-mentioned PCM1 and BBSome proteins, directly involved in centrosome maintenance and ciliogenesis.<sup>44</sup> In mammalian cells, silencing of *BBS4*, which encodes a core member of BBSome, induced PCM1 mislocalisation, concomitant de-anchoring of centrosomal microtubules, arrest in cell division and apoptotic cell death.<sup>45</sup> Interestingly, *BBS4*-depleted cells always contained replicated centrioles,<sup>45</sup> which was quite similar to abnormal signals of Centrin1 observed in spermatozoa of the *DZIP1*-mutated men (figure 4). Furthermore, the concentrated immunostaining spot of *DZIP1* was observed in normal sperm neck where sperm centrioles and pericentriolar



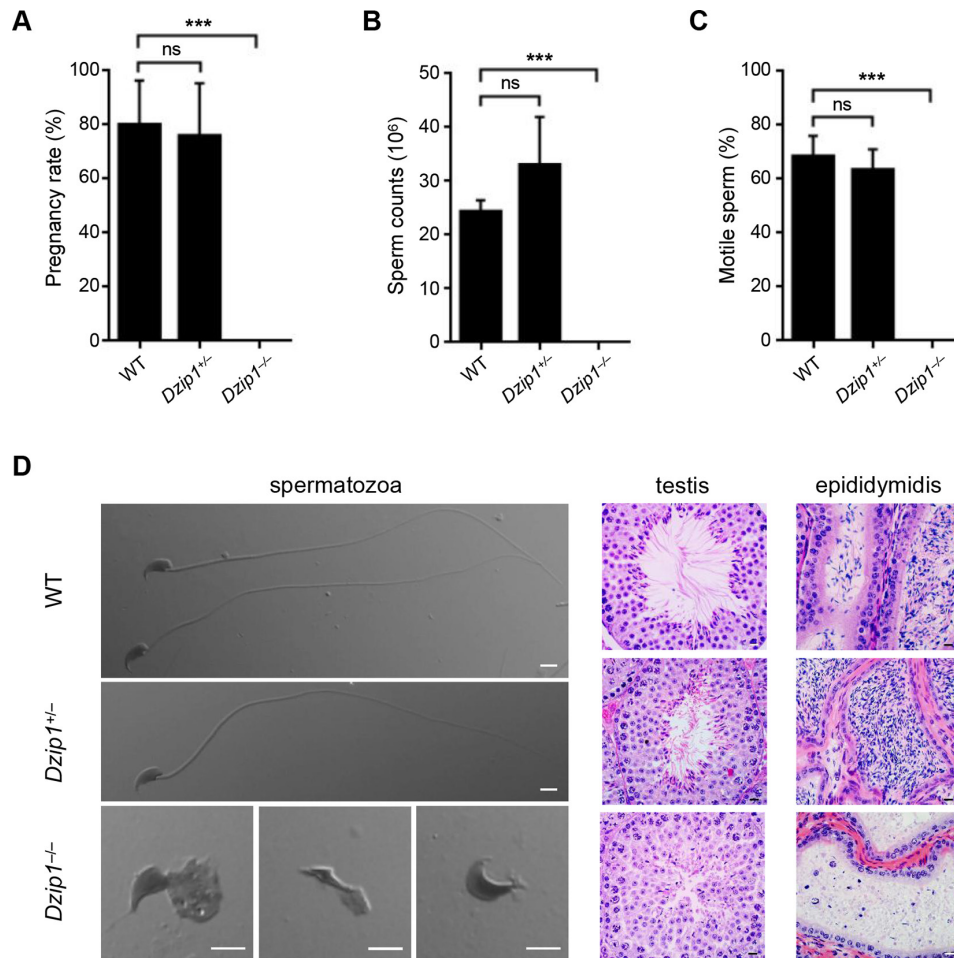


**Figure 5** Severe asthenoteratospermia phenotypes in *Dzip1*-knockout male mice. (A) The pregnancy rate of heterozygous mutated (*Dzip1*<sup>+/-</sup>) and homozygous mutated (*Dzip1*<sup>-/-</sup>) male mice. No significant difference in pregnancy rate was observed between the *Dzip1*<sup>+/-</sup> male mice and the WT male mice, but all the *Dzip1*<sup>-/-</sup> male mice were infertile. (B) Sperm counts per epididymis of *Dzip1*<sup>+/-</sup> and *Dzip1*<sup>-/-</sup> male mice. No significant difference in sperm count was observed between WT and *Dzip1*<sup>+/-</sup> male mice, whereas few spermatozoa from the epididymides of *Dzip1*<sup>-/-</sup> male mice were collected. (C) Sperm motility of *Dzip1*<sup>+/-</sup> and *Dzip1*<sup>-/-</sup> male mice. No significant difference in sperm motility was observed between WT and *Dzip1*<sup>+/-</sup> male mice. But spermatozoa from *Dzip1*<sup>-/-</sup> male mice presented no motility. (D) Sperm morphology and histological staining of WT, *Dzip1*<sup>+/-</sup> and *Dzip1*<sup>-/-</sup> male mice under light microscopy. The sperm morphology was normal in WT and *Dzip1*<sup>+/-</sup> male mice. However, most spermatozoa from *Dzip1*<sup>-/-</sup> male mice had severe malformations, such as absent flagella, cytoplasm residual and abnormal heads. In comparison to the WT and *Dzip1*<sup>+/-</sup> male mice, few spermatozoa with normal flagella were observed in seminiferous tubules and epididymis from *Dzip1*<sup>-/-</sup> male mice. Scale bar: 5 μm. abbreviation: NS, no significance; WT, wild type.

matrixes locate. Consequently, the failure of flagellar formation and the disorder of centrioles in spermatozoa of *DZIP1*-mutated individuals were probably due to the centrosomal damage caused by the absence of *DZIP1*.

It has been recently reported that, in addition to a proximal centriole, there is an atypical flagellum-attached distal centriole existing in the mature spermatozoon of fertile men.<sup>46</sup> Two immunostaining spots of Centrin1 signals observed in spermatozoa of the control subject in our study partially confirmed the existence of two centrioles in mature human sperm as well (figure 4). The distal centriole, which functions as the zygote's second centriole, is capable of recruiting pericentriolar matrixes, forming a daughter centriole, and localising to the spindle pole during mitosis, thus plays essential roles especially during the first mitosis after fertilisation.<sup>46</sup> Another recent study as to dual-spindle formation in zygotes also hinted that sperm centrioles could be associated with keeping parental genomes apart in early mammalian embryos through the participation in forming dual spindles.<sup>47</sup> Therefore, the abnormality of sperm centrioles

caused by deficiency of *DZIP1* may have important influence on subsequent fertilisation and cleavage.

Overall, in humans and mice, we found that the *DZIP1* deficiency caused by homozygous *DZIP1* mutations resulted in male infertility characterised by asthenoteratospermia with the damage of both flagellar formation and sperm centrioles, thus establishing *DZIP1* as a gene responsible for asthenoteratospermia with severe MMAF.

#### Author affiliations

<sup>1</sup>Reproductive Medicine Center, Department of Obstetrics and Gynecology, The First Affiliated Hospital of Anhui Medical University, Hefei, China

<sup>2</sup>NHC Key Laboratory of Study on Abnormal Gametes and Reproductive Tract (Anhui Medical University), Hefei, China

<sup>3</sup>Key Laboratory of Population Health Across Life Cycle (Anhui Medical University), Ministry of Education of the People's Republic of China, Hefei, China

<sup>4</sup>Obstetrics and Gynecology Hospital, NHC Key Laboratory of Reproduction Regulation (Shanghai Institute of Planned Parenthood Research), State Key Laboratory of Genetic Engineering at School of Life Sciences, Fudan University, Shanghai, China

<sup>5</sup>Shanghai Key Laboratory of Female Reproductive Endocrine Related Diseases, Shanghai, China

<sup>6</sup>State Key Laboratory of Reproductive Medicine, Center for Global Health, School of Public Health, Nanjing Medical University, Nanjing, China

<sup>7</sup>Key Laboratory of Cell Proliferation and Differentiation of the Ministry of Education, College of Life Sciences, Peking University, Beijing, China

<sup>8</sup>Anhui Province Key Laboratory of Reproductive Health and Genetics, Anhui Medical University, Hefei, China

<sup>9</sup>Anhui Provincial Engineering Technology Research Center for Biopreservation and Artificial Organs, Hefei, China

<sup>10</sup>Center for Reproduction and Genetics, The Affiliated Suzhou Hospital of Nanjing Medical University, Suzhou, China

<sup>11</sup>Genesky Biotechnologies Inc, Shanghai, Shanghai, China

<sup>12</sup>Center of Cryo-Electron Microscopy, Zhejiang University, Hangzhou, China

<sup>13</sup>Department of Pathology, The First Affiliated Hospital of Anhui Medical University, Hefei, China

<sup>14</sup>Department of Epidemiology and Biostatistics, School of Public Health, Anhui Medical University, Hefei, China

**Acknowledgements** We would like to thank the families for participating and supporting this study. We also thank the Center of Cryo-electron Microscopy at Zhejiang University for technical support.

**Contributors** YC, FZ, CZ and XH designed the study. XH, SY, HW, JW, YG, QT, DT, JIZ, BS, YZ, YX, PZ, ZW and ZZ provided patients' data and performed clinical assessments. XH, ML, WL, WC, HC, QL, XN, W-YL, JW, JuZ, YG, Y-JC, ChL, CaL, CY and HS conducted the experiments. HZ, XH, ML, WL, W-YL and FZ analysed the data. WL, RL, XH and FZ wrote the manuscript. YC and FZ were responsible for the study supervision. All authors read and approved the final manuscript.

**Funding** This study was supported by National Natural Science Foundation of China (81971441, 31625015, 81601340 and 31521003), Special Foundation for Development of Science and Technology of Anhui Province (2017070802D150), Natural Science Foundation of Anhui Province (1708085QC59 and 1908085QH313), Shanghai Medical Center of Key Programs for Female Reproductive Diseases (2017ZZ01016), the Shanghai Municipal Science and Technology Major Project (2017SHZDZX01) and Jiangsu Commission of Health (H2018050).

**Competing interests** None declared.

**Patient consent for publication** Obtained.

**Ethics approval** This study was approved by the Ethical Committees of Anhui Medical University and the School of Life Sciences at Fudan University.

**Provenance and peer review** Not commissioned; externally peer reviewed.

**Data availability statement** Data are available in a public, open access repository. Data are available upon reasonable request. All data relevant to the study are included in the article or uploaded as supplementary information. All data relevant to the study are available in public.

**Author note** YC, FZ, CZ and XH jointly direct this study.

**Open access** This is an open access article distributed in accordance with the Creative Commons Attribution Non Commercial (CC BY-NC 4.0) license, which permits others to distribute, remix, adapt, build upon this work non-commercially, and license their derivative works on different terms, provided the original work is properly cited, appropriate credit is given, any changes made indicated, and the use is non-commercial. See: <http://creativecommons.org/licenses/by-nc/4.0/>.

## ORCID iDs

Bing Song <http://orcid.org/0000-0002-7182-0175>

Xiaojin He <http://orcid.org/0000-0001-5919-8478>

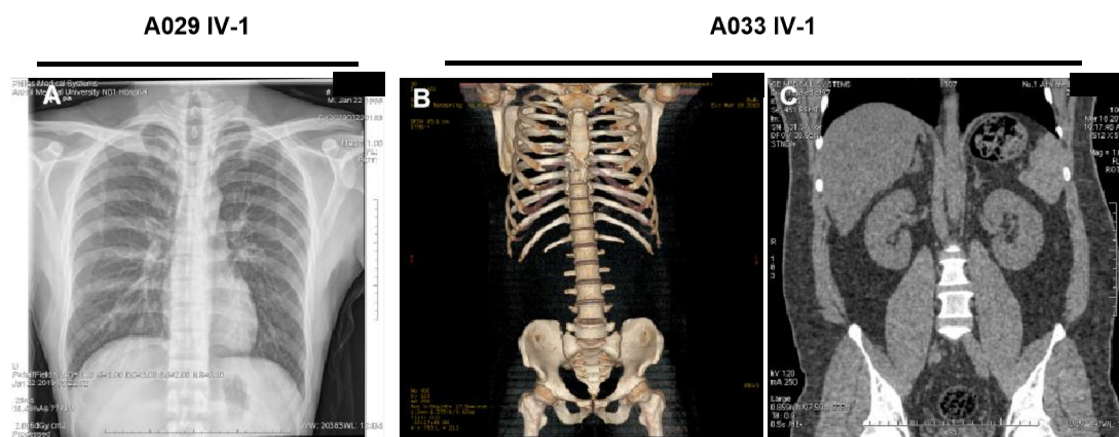
Feng Zhang <http://orcid.org/0000-0003-4556-8276>

## REFERENCES

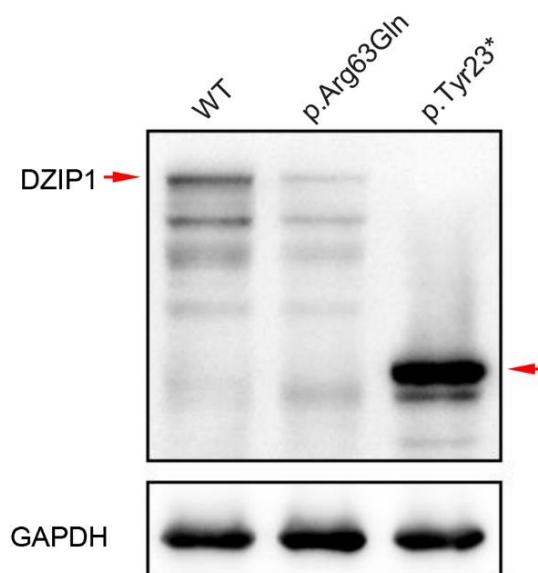
- Cocuzza M, Cocuzza MA, Bragais FMP, Agarwal A. The role of varicocele repair in the new era of assisted reproductive technology. *Clinics* 2008;63:395–404.
- Dong FN, Amiri-Yekta A, Martinez G, Saut A, Tek J, Stouvenel L, Lorès P, Karaouzen T, Thierry-Mieg N, Satre V, Brouillet S, Daneshpour A, Hosseini SH, Bonhivers M, Gourabi H, Dulioust E, Arnoult C, Touré A, Ray PF, Zhao H, Coutton C. Absence of CFAP69 causes male infertility due to multiple morphological abnormalities of the flagella in human and mouse. *Am J Hum Genet* 2018;102:636–48.
- McLachlan RI, Rajpert-De Meyts E, Hoei-Hansen CE, de Kretser DM, Skakkebaek NE. Histological evaluation of the human testis—approaches to optimizing the clinical value of the assessment: mini review. *Hum Reprod* 2007;22:2–16.
- Avidan N, Tamary H, Dgany O, Cattani D, Pariente A, Thulliez M, Borot N, Moati L, Barthelme A, Shalmon L, Krasnov T, Ben-Asher E, Olender T, Khen M, Yaniv I, Zaizov R, Shalev H, Delaunay J, Fellous M, Lancet D, Beckmann JS, Catsperz, a human autosomal nonsyndromic male infertility gene. *Eur J Hum Genet* 2003;11:497–502.
- Zhu F, Wang F, Yang X, Zhang J, Wu H, Zhang Z, Zhang Z, He X, Zhou P, Wei Z, Gez J, Cao Y. Biallelic SUN5 mutations cause autosomal-recessive acephalic spermatozoa syndrome. *Am J Hum Genet* 2016;99:942–9.
- Coutton C, Vargas AS, Amiri-Yekta A, Kherraf Z-E, Ben Mustapha SF, Le Tanno P, Wambergue-Legrand C, Karaouzen T, Martinez G, Crouzy S, Daneshpour A, Hosseini SH, Mitchell V, Halouani L, Marrakchi O, Makni M, Latrous H, Kharouf M, Deleuze J-F, Boland A, Hennebicq S, Satre V, Joux P-S, Thierry-Mieg N, Conne B, Dacheux D, Landrein N, Schmitt A, Stouvenel L, Lorès P, El Khouri E, Bottari SP, Fauré J, Wolf J-P, Pernet-Gallay K, Escoffier J, Gourabi H, Robinson DR, Nef S, Dulioust E, Zouari R, Bonhivers M, Touré A, Arnoult C, Ray PF. Mutations in CFAP43 and CFAP44 cause male infertility and flagellum defects in Trypanosoma and human. *Nat Commun* 2018;9:686.
- Baccetti B, Collodel G, Estenoz M, Manca D, Moretti E, Piomboni P. Gene deletions in an infertile man with sperm fibrous sheath dysplasia. *Hum Reprod* 2005;20:2790–4.
- Tang S, Wang X, Li W, Yang X, Li Z, Liu W, Li C, Zhu Z, Wang L, Wang L, Sun X, Zhi E, Wang H, Li H, Jin L, Luo Y, Wang J, Yang S, Zhang F. Biallelic mutations in CFAP43 and CFAP44 cause male infertility with multiple morphological abnormalities of the sperm flagella. *Am J Hum Genet* 2017;100:854–64.
- Sha Y-W, Wang X, Su Z-Y, Mei L-B, Ji Z-Y, Bao H, Li P. Patients with multiple morphological abnormalities of the sperm flagella harbouring CFAP44 or CFAP43 mutations have a good pregnancy outcome following intracytoplasmic sperm injection. *Andrologia* 2019;51:e13151.
- He X, Li W, Wu H, Lv M, Liu W, Liu C, Zhu F, Li C, Fang Y, Yang C, Cheng H, Zhang J, Tan J, Chen T, Tang D, Song B, Wang X, Zha X, Wang H, Wei Z, Yang S, Saiyin H, Zhou P, Jin L, Wang J, Zhang Z, Zhang F, Cao Y. Novel homozygous CFAP69 mutations in humans and mice cause severe asthenoteratospermia with multiple morphological abnormalities of the sperm flagella. *J Med Genet* 2019;56:106–103.
- Ben Khelifa M, Coutton C, Zouari R, Karaouzen T, Rendu J, Bidart M, Yassine S, Pierre V, Delaroché J, Hennebicq S, Grunwald D, Escalier D, Pernet-Gallay K, Joux P-S, Thierry-Mieg N, Touré A, Arnoult C, Ray PF. Mutations in DNAH1, which encodes an inner arm heavy chain dynein, lead to male infertility from multiple morphological abnormalities of the sperm flagella. *Am J Hum Genet* 2014;94:95–104.
- Wang X, Jin H, Han F, Cui Y, Chen J, Yang C, Zhu P, Wang W, Jiao G, Wang W, Hao C, Gao Z. Homozygous DNAH1 frameshift mutation causes multiple morphological anomalies of the sperm flagella in Chinese. *Clin Genet* 2017;91:313–21.
- Wambergue C, Zouari R, Fourati Ben Mustapha S, Martinez G, Devillard F, Hennebicq S, Satre V, Brouillet S, Halouani L, Marrakchi O, Makni M, Latrous H, Kharouf M, Amblard F, Arnoult C, Ray PF, Coutton C. Patients with multiple morphological abnormalities of the sperm flagella due to DNAH1 mutations have a good prognosis following intracytoplasmic sperm injection. *Hum Reprod* 2016;31:1164–72.
- Sha Y, Yang X, Mei L, Ji Z, Wang X, Ding L, Li P, Yang S. DNAH1 gene mutations and their potential association with dysplasia of the sperm fibrous sheath and infertility in the Han Chinese population. *Fertil Steril* 2017;107:1312–8.
- Martinez G, Kherraf Z-E, Zouari R, Fourati Ben Mustapha S, Saut A, Pernet-Gallay K, Bertrand A, Bidart M, Hograindeur JP, Amiri-Yekta A, Kharouf M, Karaouzen T, Thierry-Mieg N, Dacheux-Deschamps D, Satre V, Bonhivers M, Touré A, Arnoult C, Ray PF, Coutton C. Whole-Exome sequencing identifies mutations in FSIP2 as a recurrent cause of multiple morphological abnormalities of the sperm flagella. *Hum Reprod* 2018;33:1973–84.
- Liu W, Wu H, Wang L, Yang X, Liu C, He X, Li W, Wang J, Chen Y, Wang H, Gao Y, Tang S, Yang S, Jin L, Zhang F, Cao Y. Homozygous loss-of-function mutations in FSIP2 cause male infertility with asthenoteratospermia. *J Genet Genomics* 2019;46:53–6.
- Liu W, He X, Yang S, Zouari R, Wang J, Wu H, Kherraf Z-E, Liu C, Coutton C, Zhao R, Tang D, Tang S, Lv M, Fang Y, Li W, Li H, Zhao J, Wang X, Zhao S, Zhang J, Arnoult C, Jin L, Zhang Z, Ray PF, Cao Y, Zhang F. Bi-Allelic mutations in TTC21A induce Asthenoteratospermia in humans and mice. *Am J Hum Genet* 2019;104:738–48.
- Kherraf Z-E, Amiri-Yekta A, Dacheux D, Karaouzen T, Coutton C, Christou-Kent M, Martinez G, Landrein N, Le Tanno P, Fourati Ben Mustapha S, Halouani L, Marrakchi O, Makni M, Latrous H, Kharouf M, Pernet-Gallay K, Gourabi H, Robinson DR, Crouzy S, Blum M, Thierry-Mieg N, Touré A, Zouari R, Arnoult C, Bonhivers M, Ray PF. A homozygous ancestral SVA-Insertion-Mediated deletion in WDR66 induces multiple morphological abnormalities of the sperm flagellum and male infertility. *Am J Hum Genet* 2018;103:400–12.
- Li W, He X, Yang S, Liu C, Wu H, Liu W, Lv M, Tang D, Tan J, Tang S, Chen Y, Wang J, Zhang Z, Wang H, Jin L, Zhang F, Cao Y. Biallelic mutations of CFAP251 cause sperm flagellar defects and human male infertility. *J Hum Genet* 2019;64:49–54.
- Auguste Y, Delague V, Desvignes J-P, Longepied G, Gnisci A, Besnier P, Levy N, Beroud C, Megarbane A, Metzler-Guillemain C, Mitchell MJ, Calmodulin-Lof. Loss of calmodulin- and Radial-Spoke-Associated complex protein CFAP251 leads to immotile spermatozoa lacking mitochondria and infertility in men. *Am J Hum Genet* 2018;103:413–20.
- Coutton C, Martinez G, Kherraf Z-E, Amiri-Yekta A, Bogueuet M, Saut A, He X, Zhang F, Cristou-Kent M, Escoffier J, Bidart M, Satre V, Conne B, Fourati Ben Mustapha S, Halouani L, Marrakchi O, Makni M, Latrous H, Kharouf M, Pernet-Gallay K, Bonhivers M, Hennebicq S, Rives N, Dulioust E, Touré A, Gourabi H, Cao Y, Zouari R, Hosseini SH, Nef S, Thierry-Mieg N, Arnoult C, Ray PF. Bi-Allelic mutations in ARMC2 lead to severe Asthenoteratospermia due to sperm flagellum malformations in humans and mice. *Am J Hum Genet* 2019;104:331–40.



- 22 Dieterich K, Soto Rifo R, Faure AK, Hennebicq S, Ben Amar B, Zahi M, Perrin J, Martinez D, Sèle B, Jouk P-S, Ohlmann T, Rousseaux S, Lunardi J, Ray PF. Homozygous mutation of AURKC yields large-headed polyploid spermatozoa and causes male infertility. *Nat Genet* 2007;39:661–5.
- 23 Ben Khelifa M, Zouari R, Harbuz R, Halouani L, Arnoult C, Lunardi J, Ray PF. A new AURKC mutation causing macrozoospermia: implications for human spermatogenesis and clinical diagnosis. *Mol Hum Reprod* 2011;17:762–8.
- 24 Hua J, Wan Y-yang, Wan YY. Whole-Exome sequencing identified a novel mutation of AURKC in a Chinese family with macrozoospermia. *J Assist Reprod Genet* 2019;36:529–34.
- 25 Kosciński I, Elinati E, Fossard C, Redin C, Muller J, Velez de la Calle J, Schmitt F, Ben Khelifa M, Ray PF, Ray P, Kilani Z, Barratt CLR, Viville S. DPY19L2 deletion as a major cause of globozoospermia. *Am J Hum Genet* 2011;88:344–50.
- 26 Zhu F, Gong F, Lin G, Lu G. DPY19L2 gene mutations are a major cause of globozoospermia: identification of three novel point mutations. *Mol Hum Reprod* 2013;19:395–404.
- 27 Bettencourt-Dias M, Glover DM. Centrosome biogenesis and function: centrosomes brings new understanding. *Nat Rev Mol Cell Biol* 2007;8:451–63.
- 28 Kubo A, Sasaki H, Yuba-Kubo A, Tsukita S, Shiina N. Centriolar satellites: molecular characterization, ATP-dependent movement toward centrioles and possible involvement in ciliogenesis. *J Cell Biol* 1999;147:969–80.
- 29 Ou YY, Zhang M, Chi S, Matyas JR, Rattner JB. Higher order structure of the PCM adjacent to the centriole. *Cell Motil Cytoskeleton* 2003;55:125–33.
- 30 Zimmerman W, Doxsey SJ. Construction of centrosomes and spindle poles by molecular motor-driven assembly of protein particles. *Traffic* 2000;1:927–34.
- 31 Zimmerman W, Sparks CA, Doxsey SJ. Amorphous no longer: the centrosome comes into focus. *Curr Opin Cell Biol* 1999;11:122–8.
- 32 Chemes HE. Sperm Centrioles and Their Dual Role in Flagellogenesis and Cell Cycle of the Zygote. In: Schatten H, ed. *The centrosome: cell and molecular mechanisms of functions and dysfunctions in disease*. Totowa, NJ: Humana Press, 2012: 33–48.
- 33 Sathananthan AH, Kola I, Osborne J, Trounson A, Ng SC, Bongso A, Ratnam SS. Centrioles in the beginning of human development. *Proc Natl Acad Sci U S A* 1991;88:4806–10.
- 34 Schatten H, Sun QY. The functional significance of centrosomes in mammalian meiosis, fertilization, development, nuclear transfer, and stem cell differentiation. *Environ Mol Mutagen* 2009;50:620–36.
- 35 Moore FL, Jaruzelska J, Dorfman DM, Reijo-Pera RA. Identification of a novel gene, DZIP (DAZ-interacting protein), that encodes a protein that interacts with DAZ (deleted in azoospermia) and is expressed in embryonic stem cells and germ cells. *Genomics* 2004;83:834–43.
- 36 Wang C, Low W-C, Liu A, Wang B. Centrosomal protein DZIP1 regulates hedgehog signaling by promoting cytoplasmic retention of transcription factor GLI3 and affecting ciliogenesis. *J Biol Chem* 2013;288:29518–29.
- 37 Zhang B, Wang G, Xu X, Yang S, Zhuang T, Wang G, Ren H, Cheng SY, Jiang Q, Zhang C. DAZ-interacting protein 1 (Dzip1) phosphorylation by Polo-like kinase 1 (Plk1) regulates the centriolar satellite localization of the BBSome protein during the cell cycle. *J Biol Chem* 2017;292:1351–60.
- 38 Zhang B, Zhang T, Wang G, Wang G, Chi W, Jiang Q, Zhang C. GSK3 $\beta$ -Dzip1-Rab8 cascade regulates ciliogenesis after mitosis. *PLoS Biol* 2015;13:e1002129.
- 39 Wu H, Li W, He X, Liu C, Fang Y, Zhu F, Jiang H, Liu W, Song B, Wang X, Zhou P, Wei Z, Zhang F, Cao Y. Novel CFAP43 and CFAP44 mutations cause male infertility with multiple morphological abnormalities of the sperm flagella (MMAF). *Reprod Biomed Online* 2019;38:769–78.
- 40 Liu C, Lv M, He X, Zhu Y, Amiri-Yekta A, Li W, Wu H, Kherraf Z-E, Liu W, Zhang J, Tan Q, Tang S, Zhu Y-J, Zhong Y, Li C, Tian S, Zhang Z, Jin L, Ray P, Zhang F, Cao Y. Homozygous mutations in *SPEF2* induce multiple morphological abnormalities of the sperm flagella and male infertility. *J Med Genet* 2020;57:31–7.
- 41 Glazer AM, Wilkinson AW, Backer CB, Lapan SW, Gutzman JH, Cheeseman IM, Reddien PW. The Zn finger protein Iguana impacts hedgehog signaling by promoting ciliogenesis. *Dev Biol* 2010;337:148–56.
- 42 Kim H, Richardson J, van Eeden F, Ingham PW. Gli2a protein localization reveals a role for Iguana/DZIP1 in primary ciliogenesis and a dependence of hedgehog signal transduction on primary cilia in the zebrafish. *BMC Biol* 2010;8:65.
- 43 Tay SY, Yu X, Wong KN, Panse P, Ng CP, Roy S. The iguana/DZIP1 protein is a novel component of the ciliogenic pathway essential for axonemal biogenesis. *Dev Dyn* 2010;239:527–34.
- 44 Tollenaere MAX, Mailand N, Bekker-Jensen S. Centriolar satellites: key mediators of centrosome functions. *Cell Mol Life Sci* 2015;72:11–23.
- 45 Kim JC, Badano JL, Sibold S, Esmail MA, Hill J, Hoskins BE, Leitch CC, Venner K, Ansley SJ, Ross AJ, Leroux MR, Katsanis N, Beales PL. The Bardet-Biedl protein BBS4 targets cargo to the pericentriolar region and is required for microtubule anchoring and cell cycle progression. *Nat Genet* 2004;36:462–70.
- 46 Fishman EL, Jo K, Nguyen QPH, Kong D, Royfman R, Cekic AR, Khanal S, Miller AL, Simerly C, Schatten G, Loncarek J, Mennella V, Avidor-Reiss T. A novel atypical sperm centriole is functional during human fertilization. *Nat Commun* 2018;9:2210.
- 47 Reichmann J, Nijmeijer B, Hossain MJ, Eguren M, Schneider I, Politi AZ, Roberti MJ, Hufnagel L, Hiriagi T, Ellenberg J. Dual-spindle formation in zygotes keeps parental genomes apart in early mammalian embryos. *Science* 2018;361:189–93.

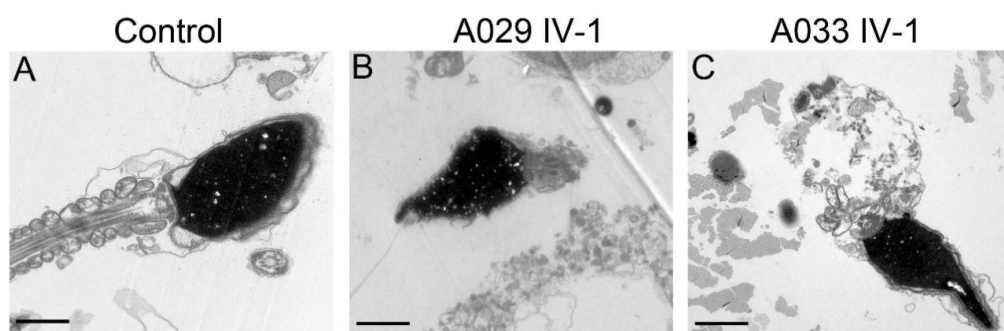


**Supplementary figure S1** Clinical examinations of the two *DZIP1*-mutated men. (A) Chest X-ray image indicated the normal pulmonary structure, heart and ribs of subject A029 IV-1. (B, C) Computed reconstructed images of the ribs, pelvis, liver and kidneys of subject A033 IV-1. No obvious abnormalities were observed. The names of the two subjects were anonymized.

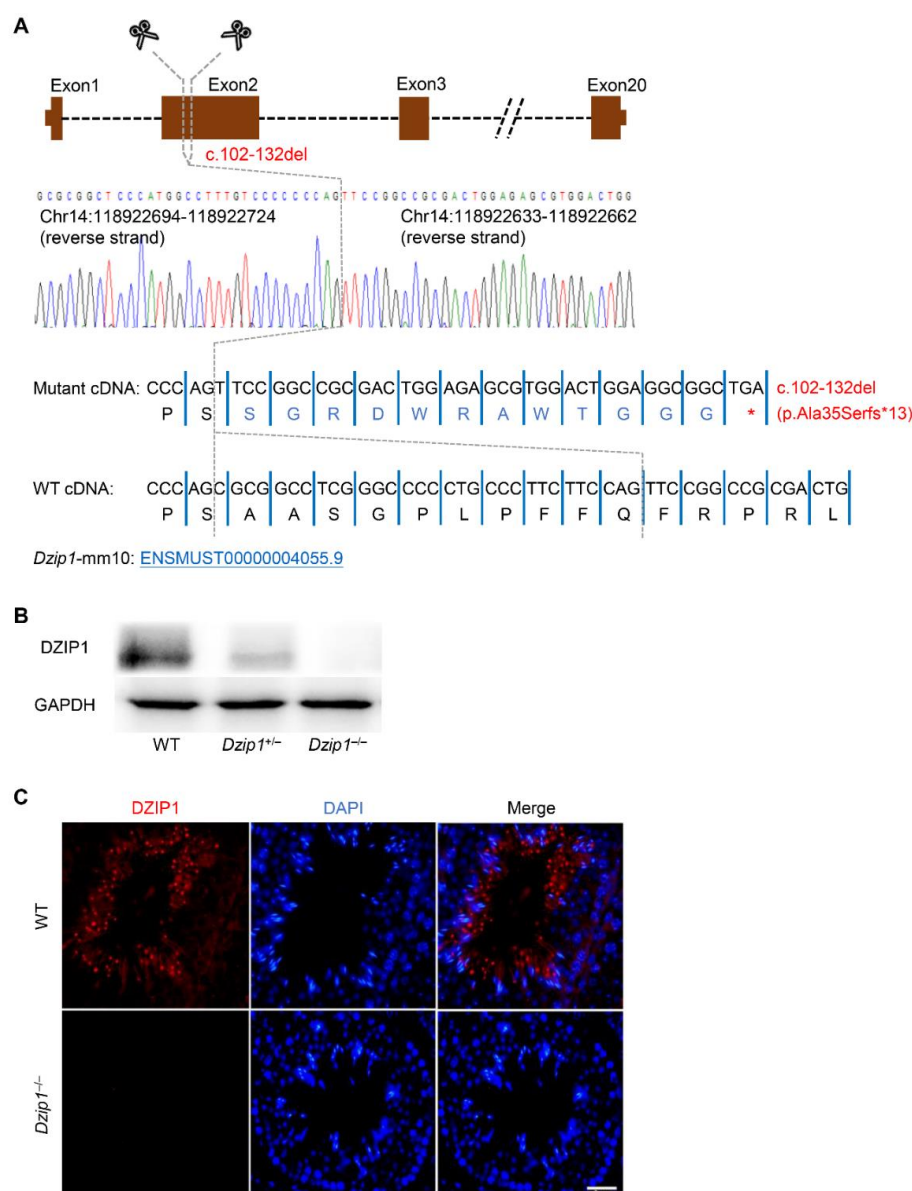


**Supplementary figure S2** Western blotting assay of the *DZIP1* mutations identified in men with asthenoteratospermia. The *in vitro* effects of the mutations on DZIP1 protein level were investigated using western blotting in HEK293T cells transfected with wild-type (WT) or *DZIP1*-mutated constructs. Red arrows: WT or mutated DZIP1 proteins.





**Supplementary figure S3** Ultra-structure of the sperm flagella from a control subject and the two *DZIP1*-mutated men. (A) The control sample showed a regular flagellum with a normal connecting piece and axoneme, which was surrounded with mitochondrial sheath. (B, C) The longitudinal section of sperm head and flagellar mid-piece of the *DZIP1*-mutated men presented with a very short axoneme structure (B) or complete lack of axoneme structure (C). Scale bar: 2  $\mu\text{m}$ .



**Supplementary figure S4** Generation of *Dzip1*-knockout mice using CRISPR-Cas9. (A) A frameshift deletion (c.102\_132del) was generated in mouse ortholog *Dzip1* using the CRISPR-Cas9 technology. This mutation was predicted to cause premature translational termination (p.Ala35Serfs\*13). (B) Western blotting analysis of the whole testis lysates from wild-type (WT), heterozygous mutated (*Dzip1*<sup>+/-</sup>) and homozygous mutated (*Dzip1*<sup>-/-</sup>) male mice. The DZIP1 protein expression levels were obviously reduced in the *Dzip1*<sup>+/-</sup> mice, and was absent in the *Dzip1*<sup>-/-</sup> mice. (C) Immunofluorescence staining of DZIP1 was conducted in mouse testicular tissues. The DZIP1 staining was detected in germ cells (especially in elongated spermatids) of the WT male mice, but was absent in the *Dzip1*<sup>-/-</sup> male mice. Scale bar: 20  $\mu$ m.

**Supplementary table S1** Primers used for amplification and verification of *DZIP1* mutations.

Primer name	Primer sequence (5'-3')	Tm
M1-F	AAGAAAGAGTGGTGATACGGGACAG	62°C
M1-R	GCCCTTCCAGAAGCATGTCTACTAC	
M2-F	AAAATGCAATCATCTTGTCAAATTC	58°C
M2-R	AAGCACCCCTGTATTATTCCTTGTTA	



**Supplementary table S2** Primers used for full-length PCR and segmental PCR.

Primer name	Primer sequence (5'-3')	Tm
WT-F	ACAAGTCCGGACTCAGATCTCCTATGCAAGCTGAGGCAGC	72°C
WT-R	TATCTAGATCCGGTGGATCCTTAGACATCTGAAGTGTCGCTC	
M1-cDNA-F	AGCTGGAGAGTGTGGACTGG	70°C
M1-cDNA-R	CAGTCCACACTCTCCAGCTGCGGCCTGAACTGGAAGAAG	
M2-cDNA-F	CAGAAAAATGCACAGATTGAG	65°C
M2-cDNA-R	CAATCTGTGCATTTTCTGCTACTCAAATGAGAATT	

**Supplementary table S3** Primers used for verification of mouse *Dzip1* mutation.

Primer name	Primer sequence (5'-3')	Tm
Mouse-F	TGCCATAGCAACGTCCTGGAC	55°C
Mouse-R	AGCTGCGAGGTGAGGAACTC	

**Supplementary table S4** Homozygous *DZIP1* mutations identified in men with asthenoteratospermia.

Individual	A029 IV-1	A033 IV-1
<i>DZIP1</i> cDNA mutation	c.188G>A	c.690T>G
Protein alteration	p.Arg63Gln	p.Tyr230*
Mutation type	missense	stop-gain
Allele frequency in human populations		
ExAC	0	0
gnomAD	0	0
1000 Genomes Project	0	0
Han Chinese controls <sup>a</sup>	0	0

<sup>a</sup> The Han Chinese controls consist of 300 fertile individuals and 668 individuals affected by non-reproductive disorders.